

Synthesis of Polypyrrole Coated SnO₂-ZnO Electrospun Nanofibers via Vapor Phase Polymerization Method

H. A. Khorami*, M. Keyanpour-Rad, A. Eghbali, M. R. Vaezi

Division of Nanotechnology and Advanced Materials, Materials & Energy Research Center

Article history:

Received 2/12/2012

Accepted 19/2/2013

Published online 1/3/2013

Keywords:

Electrospinning

Vapor Phase Polymerization

Core Sheath Nanostructure

Polypyrrole

*Corresponding author:

E-mail address:

h_a_khorami@alum.sharif.edu

Phone: +98 261 6204131

Fax: +98 261 6201888

Abstract

This paper reports the synthesis of polypyrrole coated SnO₂/ZnO electrospun nanofibers via vapor phase polymerization method. In order to prepare one dimensional (SnO₂-ZnO)/polypyrrole with the core sheath structure, first SnO₂-ZnO composite nanofibers were synthesized via electrospinning method followed by adsorption of Fe³⁺ on the surface of the SnO₂-ZnO nanofibers and finally pyrrole was polymerized on the surface of the fibers. The results of simultaneous thermal analysis (STA), X-ray diffraction (XRD), scanning electron microscopy (SEM) and transmission electron microscopy (TEM) of the nanofibers confirmed the success of synthesis of (SnO₂-ZnO)/polypyrrole core sheath compound.

2013 JNS All rights reserved

1. Introduction

Synthesis of one dimensional nanomaterials such as nanorods, nanowires, nanotubes and nanofibers have received considerable attention because of their unique properties and novel application in solar cells, catalysts, transistors and sensors devices [1-8]. Among various one dimensional nanostructure materials nanofibers, having a nanoscale diameter and microscale length, have some noticeable properties that make them an excellent candidate for many applications [5, 9-13]. One of the relatively new techniques for preparing the nanofibers is using a strong electrostatic field, namely the electrospinning

method [14]. In brief, in electrospinning a viscous polymeric or metal/polymeric solution is ejected from the needle to the target, while an electrostatic field is applied between them and a pump unlimbers a solution drop on the tip of the needle during the process. A narrow jet from the solution surface on the tip of the needle eject when the electrostatic forces overcome with the surface tension. Equilibrium condition between the electrostatic forces and surface tension on the solution drop and also the features of solution determine the morphology of the electrospinning products that it could be in the form of fiber, bead, ribbon or hollow structure [15]. Recently,

production of one dimensional organic/inorganic nanocomposite materials with combine of electrospinning and vapor phase polymerization methods has investigated extensively, mainly because of the combination of organic and inorganic materials properties and the high surface area to volume ratio of one dimensional nanomaterials [16-18]. Due to their wide direct band gap and significant electrical properties, many one dimensional metal oxides such as SnO₂ and ZnO demonstrate to be excellent candidates for variety of functional devices such as solar cells and gas sensors [19-22]. The coupled semiconductors have received great attention, because coupling the semiconductors causes some interesting developments in their properties. For example, varying the carrier mobility or decrease of the recombination rate of excitons and therefore increases the photocatalytic activity of the coupled semiconductors which make them a suitable candidate for photovoltaic applications [23]. Polypyrrole, as one of the most stable conducting polymers in ambient condition, due to its remarkable electrical, optical and photoelectric properties has been widely used in electronic devices, gas sensors and photovoltaic systems [24].

The present work reports the synthesis of (SnO₂-ZnO)/polypyrrole core sheath nanofibers from simple precursors via combination of electrospinning and vapor phase polymerization methods. The prepared nanofibers could be promising candidate for application in gas sensors and hybrid solar cells.

2. Materials

Polyvinyl alcohol (PVA) with molecular weight of ~ 72,000 g/mol (Art.No. 821038), Zinc acetate (Art. No. A769302639), Stannous chloride (Art.No. 3378443916), Iron (III) chloride (Art.No.

803945), pyrrole (Art. No. 807492) were purchased from Merck Chemical company and used as the precursors.

3. Experimental

Synthesis of (SnO₂-ZnO)/polypyrrole core sheath nanofibers were done in three steps. In the first step, the electrospinning solution was prepared by dissolving 2 g of PVA in 18 ml distilled water followed by adding 1 g zinc acetate and 1g stannous chloride to result a homogeneous, viscous and milky solution. The solution was then electrospun with the fixed distance, 6 cm, between the tip of syringe needle and Al plate collector and the feeding rate of the solution was adjusted at a constant rate of 0.2 ml/h while electric potential between the needle tip and the Al plate was maintained at 16 kV. The resulting electrospun nanofibers were then calcined at 650 °C and ambient atmosphere for 2 h, using a tube furnace, affording the SnO₂-ZnO composite nanofibers. In the second step, the SnO₂-ZnO composite nanofibers were immersed into 0.1 molar ethanoic FeCl₃ solution for 30 min followed by drying in air for 10 min to adsorb the Fe³⁺ ions on the surface of SnO₂-ZnO nanofibers, as the oxidant for polymerization process. Finally, the SnO₂-ZnO nanofibers containing the Fe³⁺ ions were exposed to saturated pyrrole vapor for 3 h to obtain (SnO₂-ZnO)/polypyrrole core sheath nanofibers. Polymerization of pyrrole monomers on the template, the SnO₂-ZnO nanofibers membrane containing the Fe³⁺ on the 1cm×1cm Al foil, was done as the following procedure. A vessel containing pyrrole which connected to an electric motor and placed on the stirrer was used while the templates were hanging up into vessel. The pyrrole stirred and heated for 3 h to polymerizing pyrrole

monomers on template while the electric motor was helping the vaporization process.

Thermogravimetric-differential thermal analysis (TG-DTA, PLSTA 1640) was used for obtaining suitable calcination temperature. X-ray diffraction (XRD, Philips X-ray Diffractometer PW3710) analysis was used for surveying the impurity and phase characteristics of the electrospun nanofibers. The surface morphology of the electrospun nanofibers and polypyrrole coated nanofibers were studied using a Philips XL30 Scanning Electron Microscope (SEM). Transmission Electron Microscopy (TEM) was used for investigating polypyrrole coating.

4. Results and discussion

The thermal behavior of the electrospun nanofibers were studied by TGA and DTA analyses. Fig.1 depicts the TGA and DTA curves resulting from the measurements performed on the electrospun nanofibers. The TGA curve exhibits two apparent mass losses. The first one between 170 °C and 240 °C is likely due to the loss of residual solvent and water remaining in the nanofibers, as evidenced by the exothermic peak in the DTA curve at the same temperature range. The second mass loss, which occurred between 530 °C and 650 °C, is due to evaporation of the organic chains belonging to PVA, CH₃COO group of zinc acetate and also the other volatile species such as stannous chloride. A strong exothermic peak at 630 °C in the DTA curve confirms the phase transformation from the amorphous phase to crystalline state. Therefore, based on the TG-DTA curves the temperature of 650 °C was selected as the calcination temperature in the procedure.

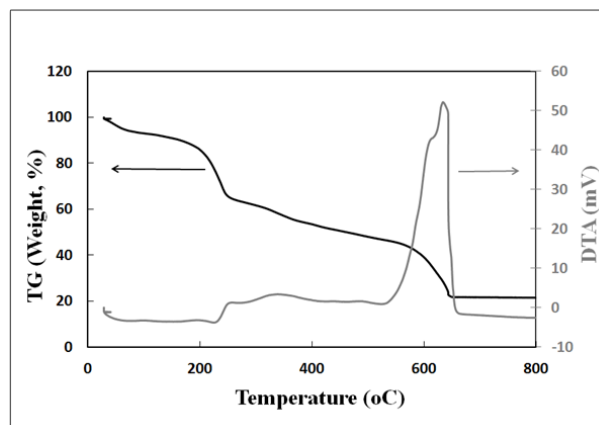


Fig. 1. Thermal behavior profile of SnO₂-ZnO electrospun nanofibers obtained from TG-DTA.

Fig. 2 shows XRD pattern of nanofibers calcined at 650 °C for 2 h. As it is shown, the existence of the sharp peaks in this figure indicates that the composite nanofibers have a polycrystalline nature with high degree of crystallinity. All diffraction peaks are attributed to various diffraction plans of SnO₂ with tetragonal rutile structure and ZnO with hexagonal wurtzite structure. The pattern also confirmed that, there are no characteristics peaks indicating presence of impurities.

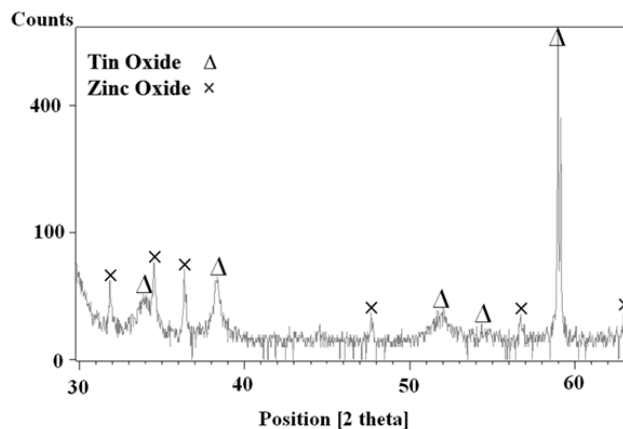


Fig. 2. XRD pattern of SnO₂-ZnO nanofibers.

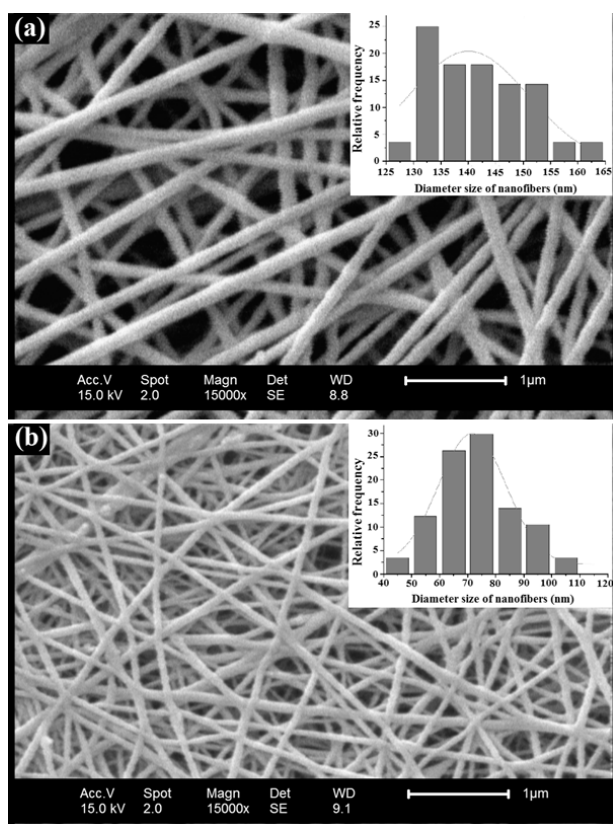


Fig. 3. SEM images of $\text{SnO}_2\text{-ZnO}$ nanofibers (a) before calcination, the inset shows distribution of nanofiber's diameter size and (b) after calcinations; the inset shows distribution of nanofiber's diameter size.

The $\text{SnO}_2\text{-ZnO}$ nanofibers were electrospun with different feeding rate, distance between the syringe needle and collector, voltage and PVA concentration, the last one also means different ratio between the zinc acetate/stannous chloride and PVA. All of these parameters affect the equilibrium condition between the electrostatic forces and the surface tension on the Taylor cone and at last, PVA concentration also affects the viscosity of the solution that these are observable from the stability of the Taylor cone and its shape during the electrospinning process. Equilibrium condition between the electrostatic forces and surface tension, and the solution behavior, e.g. solution viscosity, determine the morphology of the electrospinning products that it can be in the

form of fiber, bead or ribbon. Nanofibers structure does not have beads and ribbons when the Taylor cone is stable and conoid during the electrospinning process. Therefore, the optimum quantities of the parameters should be obtained to reach the favorable structure of fibers having any beads and ribbons. The optimum PVA concentration and electrospinning voltage were obtained 10 wt% and 16kV, respectively while the best feeding rate and distance between the syringe needle and collector were obtained 0.2 ml/h and 6 cm, respectively. Fig.3a and 3b show the SEM micrographs of electrospun nanofibers before and after calcination, respectively. As Fig.3 indicates, there are no beads and ribbons in the nanofibers membrane that it demonstrates the parameters of electrospinning process which were selected in this experiment are the optimum parameters. As it is shown in Fig.3, nanofibers have smooth edges and are randomly distributed. The diameter of the nanofibers can change to thinner fibers due to removal of the volatile species and decomposition of precursor to metal oxides during the calcination process but the texture of calcined nanofibers is kept unchanged (see Fig.3b). As shown in the inset of Fig.3b, the majority of the calcined nanofibers diameter sizes fall into the range of 60- 80 nm having average size of about 75 nm, while the inset of Fig.3a shows that, the average size of the nanofibers diameter before the calcination process was about 147 nm. Also, from Fig.2 and Fig.3b it can be concluded that the time of calcination is long enough for the process, because in the longer time the nanofibers break up while in the shorter time the XRD peaks of the nanofibers are not sharp enough to confirm high crystallinity of the nanofibers (see Fig.2). The selected time of calcination was also confirmed by observing

unbroken nanofibers in the SEM micrograph of the fibers after calcination (see Fig.3b).

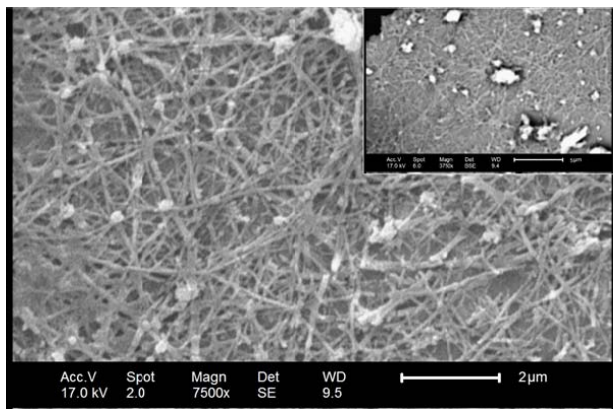


Fig. 4. SEM image of $(\text{SnO}_2\text{-ZnO})/\text{polypyrrolenanofibers}$, the inset shows the back scattered electron mode of SEM image of $(\text{SnO}_2\text{-ZnO})/\text{polypyrrolenanofibers}$.

Fig. 4 shows the SEM micrograph of $(\text{SnO}_2\text{-ZnO})/\text{polypyrrole}$ core sheath nanofibers. As shown in this figure the morphology of the $(\text{SnO}_2\text{-ZnO})/\text{polypyrrolenanofibers}$ are similar to the morphology of the $\text{SnO}_2\text{-ZnO}$ nanofibers. Furthermore, there are some white regions in this image that are attributed to aggregation of polypyrrole and they are also clearly observed in the back scattered electron mode of SEM micrograph (see inset of Fig.4). In Fig.4 $\text{SnO}_2\text{-ZnO}$ shows up as the darker regions as a consequence of a higher electron density. Despite showing the morphology of $(\text{SnO}_2\text{-ZnO})/\text{polypyrrolenanofibers}$ in the SEM image, the polypyrrole layer did not reveal in it (see Fig.4), and therefore, the TEM analysis was done to examine the polypyrrole layer.

Fig. 5 shows the TEM image of $(\text{SnO}_2\text{-ZnO})/\text{polypyrrolenanofibers}$. As shown in Fig.5, polypyrrole coated nanofibers has a core sheath structure and the ultrathin polypyrrole layer could be seen in it, with about 5-7 nm thickness. Also,

the core of $(\text{SnO}_2\text{-ZnO})/\text{polypyrrolenanofibers}$, which is seen in this image, is about 70-80 nm, confirming the nanofibers diameter size measurements which was derived from SEM images.

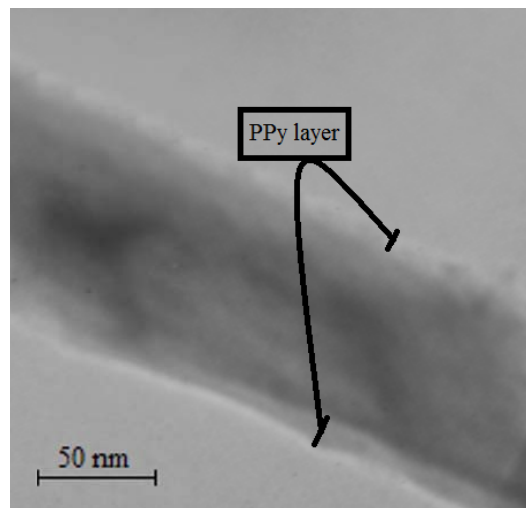


Fig. 5. TEM image of $(\text{SnO}_2\text{-ZnO})/\text{polypyrrolenanofibers}$.

Furthermore, color changes in the polymerization process were evidence, confirming that the polymerization and formation of ultrathin polypyrrole layer was done correctly. Although the original $\text{SnO}_2\text{-ZnO}$ nanofibers had a white color, the $\text{SnO}_2\text{-ZnO}$ nanofibers that immersed into ethanoic solution of FeCl_3 and dried in air became yellowish. When the sample was exposed to pyrrole vapor, the changing color from yellow to black could be seen as a sing of polypyrrole formation on the surface of the nanofibers.

5. Conclusion

The $(\text{SnO}_2\text{-ZnO})/\text{polypyrrolenanofibers}$ with the core sheath structure were synthesized via combination of electrospinning and vapor phase polymerization methods. For this purpose, the highly porous structure of $\text{SnO}_2\text{-ZnO}$ nanofibers with the smooth edges, good distribution of

diameter size, average diameter size of about 75 nm and high surface area to volume ratio were synthesized by electrospinning method and then polypyrrole was polymerized on the nanofibers surface by vapor phase polymerization method. The thickness of polypyrrole layer was about 5-7 nanometers so that the carriers could tunnel through it to the semiconductor core. The properties of synthesized nanofibers make them an excellent candidate for application in gas sensors and photovoltaic cells.

References

- [1] W.U. Huynh, J. J. Dittmer, A. Paul Alivisatos, *Science* 295 (2002) 2425.
- [2] S. Ju, J. Li, N. Pimparkar, M.A. Alam, R. P. H. Chang, David B. Janes, *IEEE Transactions on nanotechnology* 6 (2007) 390.
- [3] Y. SeokKim, B.-K. Yu, D.-Y. Kim, W.B. Kim, *Solar Energy Materials & Solar Cells* 95 (2011) 2874.
- [4] G. Rosaz, B. Salem, N. Pauc, P. Gentile, A. Potié, T. Baron, *Microelectronic Engineering* 88 (2011) 3312.
- [5] Fangli Yuan, HyungKyun Yu, HojinRyu, *ElectrochimicaActa* 50 (2004) 685.
- [6] Zhen-gang Zhao, Xiao-wei Liu, Wei-ping Chen, Tuo Li, *Sensors and Actuators A* 168 (2011) 10.
- [7] V. V. Kislyuk, O. P. Dimitriev, *Nanoscience and Nanotechnology* 8 (2008) 131.
- [8] Q. Liu, Z. Yan, N. L. Henderson, J. Chris Bauer, D. W. Goodman, J. D. Batteas, R. E. Schaak, *J. Am. Chem. Soc.* 131 (2009) 5720.
- [9] Z.-M. Huang, Y.-Z. Zhang, M. Kotaki, S. Ramakrishna, *Composites Science and Technology* 63 (2003) 2223.
- [10] P. W. Gibson, C. Lee, F. Ko, Darrell Reneker, *Engineered Fibers and Fabrics* 2 (2007) 32.
- [11] Quynh P. Pham, Upma Sharma, Antonios G. Mikos, *Tissue Engineering* 12 (2006) 1197.
- [12] Bin Ding, Moran Wang, Jianyong Yu, Gang Sun, *Sensors* 9 (2009) 1609.
- [13] Jianjun Miao, Minoru Miyauchi, Trevor J. Simmons, Jonathan S. Dordick, Robert J. Linhardt, *Nanoscience and Nanotechnology* 10 (2010) 5507.
- [14] Andreas Greiner, Joachim H. Wendorff, *AngewandteChemie International Edition* 46 (2007) 5670.
- [15] W E Teo, S Ramakrishna, *Nanotechnology* 17 (2006) 89.
- [16] X. Lu, Q. Zhao, X. Liu, D. Wang, W. Zhang, C. Wang, Y. Wei, *Macrom. Rap. Commun.* 27 (2006) 430.
- [17] Y. Wang, W.a, Timothy Strout, AshelySchempf, Heng Zhang, Baikun Li, Junhong Cui, Yu Lei, *Electroanalysis* 21 (2009) 1432.
- [18] Ying Wang, WenzhaoJia, Timothy Strout, Yu Ding and Yu Lei, *Sensors* 9 (2009) 6752.
- [19] I-Doo Kim, Jae-Min Hong, Byong Hong Lee, Dong Young Kim, Eun-Kyung Jeon, Duck-Kyun Choi, Dae-Jin Yang, *Appl.Phys. Lett.* 91 (2007) 163109.
- [20] Y. Wang, I. Ramos, J. J. Santiago-Avilés, *Appl. Phys.* 102 (2007) 093517.
- [21] J. Moon, J.A.Park, S.J. Lee, T. Zyung, *ETRI Journal* 31 (2009) 636.
- [22] Dae-Jin Yang, ItaiKamienchick, Doo Young Youn, Avner Rothschild, I-Doo Kim, *Adv. Func. Mat.* 20 (2010) 4258.
- [23] B. Attaf “Advances in composite materials for medicine and nanotechnology”, first ed., Chapter 13 by M. R. Vaezi, pp. 367-375, InTech, Rijeka, 2011.
- [24] L.X. Wang, X. G. Li, Y-L. Yang, *Reactive & Func. Poly.* 47 (2001) 125.